RESEARCH PAPER

Integrated microfluidic preconcentrator and immunobiosensor

Sowmya Kondapalli · John T. Connelly ·
Antje J. Baeumner · Brian J. Kirby

Abstract We present a microfluidic biosensor that integrates membrane-based preconcentration with fluorescence detection. The concentration membrane was fabricated in polyacrylamide by an in situ photopolymerization technique at the junction of glass microchannels. Liposomes entrapping sulforhodamine B dye molecules were used for signal amplification. The biotin–streptavidin binding system was a model system for evaluating device performance. Biotinylated liposomes were preconcentrated at the membrane by applying an electric field across the membrane. The electric field causes the liposomes to migrate toward the membrane where they are concentrated by a sieving effect. Two orders of magnitude concentration was achieved after applying the electric field for only 2 min. The concentrated bolus was then eluted toward the detection unit, where the biotinylated liposomes were captured by immobilized streptavidin. The integrated system with the preconcentration module shows a 14-fold improvement in signal as opposed to a system that does not include preconcentration.

Keywords Microfluidic biosensor · Preconcentration · Porous membrane · Liposomes

S. Kondapalli · B. J. Kirby (✉)
Sibley School of Mechanical and Aerospace Engineering,
Cornell University, Ithaca, NY 14853, USA
e-mail: kirby@cornell.edu

J. T. Connelly · A. J. Baeumner
Department of Biological and Environmental Engineering,
Cornell University, Ithaca, NY 14853, USA

1 Introduction

Microfluidic systems have become increasingly popular in biological and chemical analyses owing to the advantages of minimal reagent use, cost-effectiveness, and automation (Arora et al. 2010; Ohno et al. 2008). An important application of microfluidic systems has been in the field of biosensors for pathogen detection and clinical diagnostics (Mairhofer et al. 2009; Liu and Mathies 2009; Chen et al. 2007). However, the use of microfluidic devices for the total analysis of a whole sample has been limited owing to the challenges associated with integration of the different processing steps like sample preparation, preconcentration, analysis, and detection on the same device (Beyor et al. 2009; Sista et al. 2008; Herr et al. 2007; Easley et al. 2006; Lagally et al. 2004). In this article, we present an integrated microfluidic immunobiosensor that combines preconcentration and fluorescence detection steps to enable sensitive detection in dilute samples.

Preconcentration of sample prior to analysis is an important step in microfluidic systems as it enables detection of very small concentrations of analytes and also improves detection sensitivity and signal-to-noise ratios. A number of preconcentration techniques have been developed that can achieve high concentration factors in small time durations. Some examples include surface-binding techniques like solid-phase extraction (Jemere et al. 2002; Ramsey and Collins 2005; Yu et al. 2001) and electrokinetic manipulation techniques like isoelectric focusing (Li et al. 2003; Tan et al. 2002; Cabrera and Yager 2001), field-amplified sample stacking (Jung et al. 2003; Lichtenberg et al. 2001), isotachophoresis (Jung et al. 2006; Wainright et al. 2002; Wang et al. 2009), and dielectrophoresis (Lapizco-Encinas et al. 2005; Moncada-Hernandez and Lapizco-Encinas 2010). However, the limitations of

Fig. 1 Image of the integrated glass microfluidic device used for the biotin–streptavidin experiments, with the channels filled with food dye to show contrast. The *inset* shows a picture of the polyacrylamide membrane-based concentrator at the junction of microchannels. Biotinylated liposomes are captured by streptavidin-conjugated magnetic beads localized at the magnet. The fluorescence from the lysed liposomes is imaged downstream from the magnet in the region marked as the fluorescence measurement window
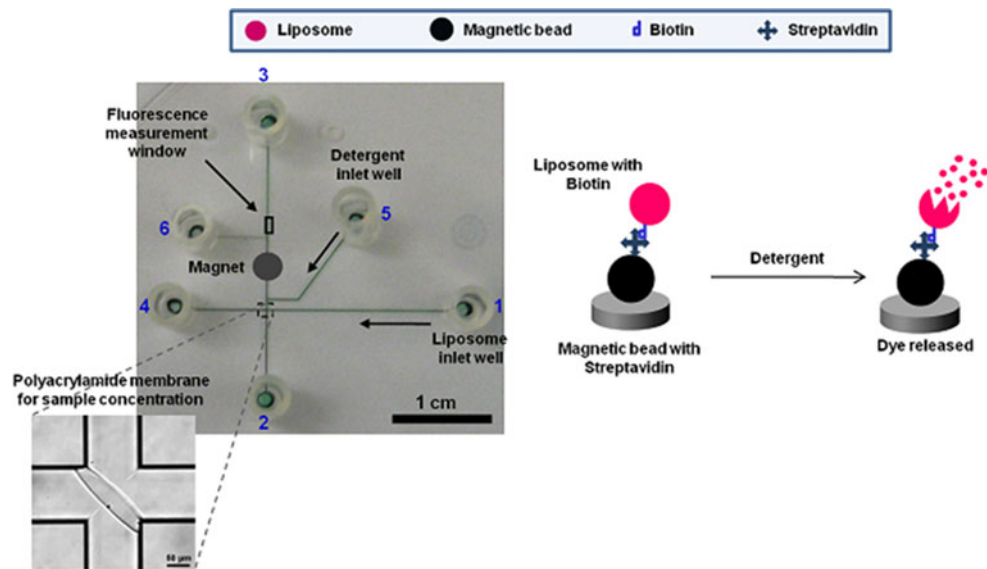
these techniques are that they either involve buffer handling challenges or fabrication complexities making them difficult to integrate with lab-on-chip systems. Porous membrane-based preconcentration systems, on the other hand, do not require complex buffer systems to concentrate samples. Khandurina et al. (1999; Foote et al. 2005) demonstrated the use of a porous silicate membrane and Wang et al. (2005) used a nanofluidic filter for preconcentration. However, in the former case, the authors reported that the silicate membranes were hard to fabricate in a reproducible manner and the latter approach involves the fabrication of micro- and nanochannels in the same device. More recently, Kim et al. (Kim and Han 2008) have developed self-sealed nanoporous junctions inside PDMS microchannels for preconcentration. However, PDMS-based devices are less robust than glass-based microfluidic devices and are prone to surface adhesion and reusability issues.

We use an in situ photopolymerized nanoporous membrane (Song et al. 2004a, b; Hatch et al. 2006) in our integrated glass microfluidic device for the preconcentration step. Song et al. (2004a) have shown high concentration factors (four orders of magnitude local concentration) using these nanoporous membranes. The in situ fabrication technique allows for easy integration with total analysis systems. Our membranes are fabricated in polyacrylamide as it is hydrophilic, biocompatible, and shows minimal non-specific adhesion (Hatch et al. 2006). The pore size of acrylamide gels can be easily adjusted by changing the percentage of monomer components (Holmes and Stellwagen 1991a, b). Moreover, unlike other membrane-based concentration methods, the response of this system is linear with the voltage–time product (Song et al. 2004a).

Figure 1 shows the integrated microfluidic biosensor with the inset showing the concentration membrane. The membrane is nanoporous and is made using polyacrylamide at the intersection of the glass channels by an in situ photopolymerization technique (Hatch et al. 2006; Song et al. 2004a, b). We use liposomes, which can encapsulate a very large number of fluorescent dye molecules in their core for signal amplification in the biosensor. Fluorescence from the dye molecules is quenched when they are encapsulated at a high concentration within the liposome core. The analytes to be detected are tagged with liposomes (Edwards et al. 2008) and these complexes are injected into the inlet well of the device. An electric field is applied across the membrane, causing the liposome–analyte complexes to migrate toward the membrane. However, since the size of the pores in the membranes is much smaller than the size of these complexes, they are concentrated at the membrane by a sieving effect. The concentrated bolus is then eluted toward the detection region, where these complexes are captured using immobilized antibodies. The captured liposomes are then lysed by flowing a detergent and the released fluorophores result in a significant signal enhancement due to the elimination of self-quenching of the dye molecules.

In this article, we present results showing improved detection sensitivity with the inclusion of the preconcentration system using proof-of-concept experiments performed with biotin–streptavidin binding.

2 Experimental methods

2.1 Fabrication of microfluidic channels

Schott D263 glass wafers (100 mm diameter, 0.55 mm thick; S I Howard Co., Worcester, MA) were used for

etching microfluidic channels. Device geometry was defined using L-Edit CAD software (Tanner Research) and a photomask was created using GCA/Mann 3600F Optical Pattern Generator. A 225-nm thick layer of amorphous silicon deposited on the glass wafers by PECVD was used as the hard mask for etching. The wafers were then coated with a 3-μm layer of Shipley 1818 positive photoresist and soft-baked at 115°C for 1 min. The mask pattern was transferred to the photoresist using an EV 620 contact aligner and the wafers were developed using a 300MIF resist developer. The exposed silicon was etched using an Oxford 80 (#1) reactive ion etching (RIE) system and the photoresist was stripped by a mixture of acetone and iso-propanol. The exposed glass was etched using a 16% HF solution (Shape Products Company, Oakland, CA). The glass wafers were exposed to HF for 14 min, resulting in channel depths of 20 μm (etch rate of D263 glass in 16% HF is about 1.4 μm/min when left unagitated). Finally, the remaining silicon on the wafers was removed by RIE using the Oxford 80 (#1) system. In the final device, the wide channel width was 120 μm and the narrow channel width was 50 μm. The depths of the channels in both cases were 20 μm. Connection holes were made in the wafers by sandblasting.

2.2 Wafer bonding

The glass microchannels were sealed by a plain borofloat glass wafer (100 mm diameter, 500 μm thick; Mark Optics, Santa Ana, CA) using a low temperature glass bonding technique (Wang et al. 1997; Khandurina et al. 1999, 2000; Foote et al. 2005). The etched and the plain glass wafers were cleaned by sonicating in acetone for about 5 min. The wafers were then hydrolyzed in RCA cleaning solution (prepared by mixing 5 N ammonium hydroxide, 30% w/w hydrogen peroxide and deionized water in 3:2:9 ratio by volume) for 20 min at 70–80°C, rinsed in deionized water and dried under nitrogen. This was followed by plasma cleaning to activate the surfaces of both the wafers prior to bonding. A thin layer of potassium silicate (KASIL 2130, The PQ Corp., Valley Forge, PA) was coated on the plain glass wafer by spinning a diluted solution (1:10 by weight in deionized water) at 2000 rpm for 8 s. As the spin-coated wafer was then brought into contact with the etched glass wafer, the bonding region spread instantaneously across the entire area of the wafers. The bonded wafers were then placed in a hot press at 90°C for an hour to reinforce the bonding.

2.3 Membrane fabrication and surface treatment

The channels of the bonded devices were treated with 1 M NaOH for 20 min to remove the potassium silicate layer in the microchannels. The wafers were then rinsed with DI water and dried in nitrogen. Prior to membrane fabrication, the glass channels were coated with an acrylate-terminated self-assembling monolayer to enable covalent attachment of the polyacrylamide membrane to the channel walls (Kirby et al. 2003; Hjerten 1967, 1985). For this, the channels were prepared by exposing to 1 M HCl for 30 min, rinsing in DI water, and then exposing to 1 M NaOH for 30 min. The channels were thoroughly rinsed with DI water and then exposed to a freshly mixed coating solution containing 2:3:5 mixture (by volume) of 3-(tri-methoxysilyl)propyl acrylate, glacial acetic acid and deionized water for exactly 30 min. The channels were finally rinsed in 1-propanol and DI water and dried with vacuum.

The polyacrylamide membrane was fabricated at the intersection of the glass microchannels by a photopoly-merization technique (Hatch et al. 2006; Song et al. 2004a, b). For this, a 355-nm laser beam was shaped using a train of lenses and mirrors into a long narrow beam to match the dimensions of the channel junction. The optical train also helps to direct the beam through a microscope to enable visualization of the polymerization process. The channels were filled with a freshly prepared and degassed solution of 22% (15.7:1) acrylamide/bisacrylamide containing 0.2% (w/v) VA-086 photoinitiator (Hatch et al. 2006). All the reservoirs were capped with tape to prevent evaporation, and the solution was allowed to equilibrate for 20 min to eliminate pressure-driven flow. The membrane was then fabricated by directing the shaped laser beam toward the junction and exposing for approximately 15 s. The unpolymerized acrylamide solution was purged from the channels and the channels were rinsed thoroughly with DI water.

Finally, the channels were coated with linear poly-acrylamide to suppress the electroosmotic flow (Kirby et al. 2003; Hjerten 1967, 1985). The channels were filled with a degassed solution of 50 mg/ml acrylamide in deionized water containing 250 ppm hydroquinone and 2 mg/ml V-50 photoinitiator and exposed to UV light in a UV oven for 30 min. The unpolymerized solution was rinsed out of the channels and the channels were cleaned with DI water.

2.4 Liposome and magnetic bead preparation

Liposomes were prepared by a modified version (Edwards et al. 2008) of the reversed-phase evaporation technique described by Siebert et al. (1993). All lipids used were obtained from Avanti Polar Lipids (Alabaster, AL). Fluo-rescent liposomes encapsulate 150 mM sulforhodamine B (SRB) dye in 0.02 M HEPES, pH 7.5 in the core and also contain 0.33 mol% dipalmitoyl phosphoethanolamine-rhodamine in the bilayer. Biotinylated lipids were used in

the preparation of the liposomes in order to add functionality to the outer surface of the bilayer. The remainder of the bilayer consists of 35 mol% dipalmitoyl phosphatidylcholine, 15 mol% dipalmitoyl phosphatidylglycerol, 42 mol% cholesterol, and 6 mol% N-(glutaryl)-1,2-dipalmitoyl-sn-glycero-3-phosphoethanolamine. After formation of the vesicles, extrusions through 1 and 0.4 μm filters was performed to assure unilamellar liposomes with a uniform size distribution. Removal of unencapsulated SRB was facilitated by application of the liposome preparation to a Sephadex G-50 column equilibrated with 0.01 M HEPES, 0.2 M NaCl, 0.2 M sucrose, 0.01% sodium azide (NaN$_3$), pH 7.5 (1× HSS), also used for elution. Fractions containing liposomes were collected and dialyzed 1× HSS in the dark overnight.

To capture these biotinylated liposomes in the microfluidic device, commercially available streptavidin-conjugated superparamagnetic beads (Dynabeads MyOne Streptavidin, 1 μm in diameter; Invitrogen, Carlsbad, CA) were used. Prior to use, the stock was vortexed to homogenize the suspension and the necessary volume was removed. In order to remove preservatives and introduce the working buffer, the beads were then washed twice with an equal volume of 1× HSS by applying the tube to a magnet rack, removing the supernatant, and resuspending.

2.5 Sample loading, concentration, and detection

Prior to performing concentration and detection experiments, the channels of the device were primed with 1× HSS buffer. A permanent magnet was positioned on the top surface of the device upstream of the detection region using adhesive putty. 1 μl of Dynabeads MyOne streptavidin-conjugated superparamagnetic beads prepared in 1× HSS buffer was injected toward the magnet through the port 5 (Fig. 1) using a syringe pump at a flow rate of 1 μl/min. For the electrokinetic concentration experiments, a solution of 10,000× diluted fluorescent liposomes (biotinylated with SRB dye in the core) in 1× HSS buffer was used. For the direct injection experiments, the liposome solution was further diluted by a factor of 10 in 1× HSS buffer (due to lowest achievable flow rate limitations with our existing equipment) so that the same number of liposomes is flowed through the device for performance comparison.

For the direct injection experiments, the biotinylated liposome solution in 1× HSS buffer was injected toward the magnet with a syringe pump at a flow rate of 10 μl/h for 90 s through inlet port 1 (Fig. 1). On the other hand, for the electrokinetic concentration experiment, all the wells were filled with 60 μl of plain 1× HSS buffer except the inlet well which was filled with the liposome–HSS solution. The pressure-driven flow in the system was eliminated by adjusting the heights of the solutions in the wells. The

liposomes were then electrophoretically concentrated at the membrane by applying a voltage difference of 150 V across the membrane. After concentrating for a duration of 90 s, the concentrated bolus of liposomes was eluted toward the bead bed by applying a voltage of 150 V to the outlet port 3 downstream of the magnet. In both cases, after liposome injection, wash buffer was injected at a flow rate of 20 μl/h to wash off any unbound liposomes in the device through port 5. A detergent solution of 60 mM octyl-β-D-glucopyranoside (OG) was then flowed through the same port 5 toward the bead bed at a flow rate of 40 μl/h and the emitted fluorescence from the lysis of the liposomes was recorded downstream of the bead bed.

For each experiment, the background was calculated as the average of the total fluorescence intensity values estimated in the region of interest during the first 60 frames of the detergent injection videos.

After each run, the device was thoroughly rinsed with deionized water multiple times followed by a final rinse which involves flowing deionized water at a rate of 2 μl/min with a syringe pump for 15 min.

Concentration factors during the experiments were estimated analytically as the ratio of the swept volume of liposomes at a given electrophoretic velocity to the volume of the measurement window around the membrane. The electrophoretic velocity of liposomes was estimated from Zetasizer measurements.

3 Results

3.1 Electrophoretic concentration of fluorescent liposomes

Concentration and elution experiments were performed using fluorescent liposomes to estimate the concentration factors for the membrane-based preconcentration system. Figure 2 shows snapshots of the channel junction during the concentration and elution steps achieved by switching electric fields between the vertical and horizontal channels. Figure 3 shows the concentration factor plotted as a function of time during which the high voltage is applied across ports 1 and 4 (Fig. 2a). It can be seen from Fig. 3 that after a concentration time of 160 s, the estimated concentration factor was around 230. Analytical calculations (as described in the materials and methods section) resulted in concentration factors of around 350 for 160 s of applying high voltage which is on the same order of magnitude as the experimental value. For these calculations, the zeta potential of the liposomes estimated from Zetasizer measurements was -28.8 ± 2.9 mV (resulting in a mean electrophoretic velocity of 103.1 μm/s), while the inferred zeta potential from the experiments was −19 mV. The trend in
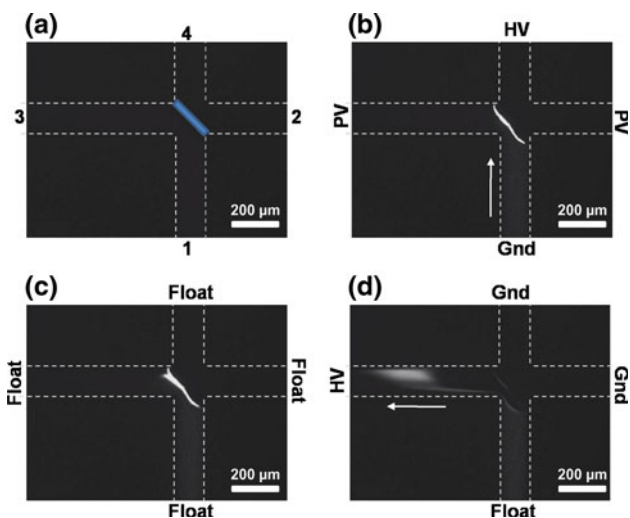
Fig. 2 Image sequence showing liposome concentration and elution. Microchannel edges have been drawn for clarity. The membrane has also been highlighted in (a). *HV* high voltage (100 V), *PV* pinch voltage (40 V), *Gnd* ground. a Before loading; b Sample concentration; c After concentration; d Sample elution. Pinch voltage is applied to minimize the diffusion of the sample away from the membrane

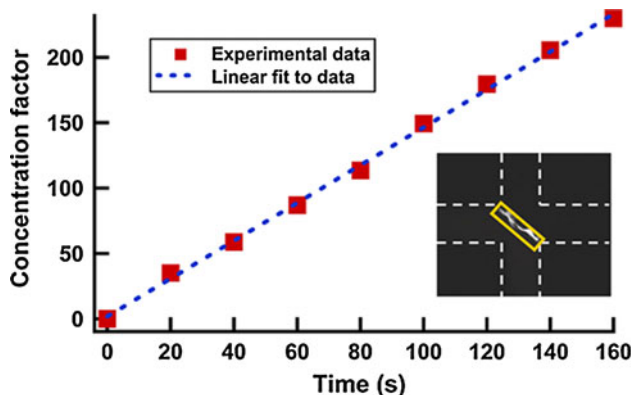Fig. 3 Concentration factors during liposome concentration as a function of time. The intensities were averaged over a measurement window (23×180 pixels) shown as a *box* in the *inset*. The concentration factors are consistent with analytical values estimated using a liposome zeta potential of -19 mV

Fig. 3 is linear, as expected, as the liposomes migrate with a constant electrophoretic velocity.

3.2 Integrated concentration and detection experiments

Concentration and detection experiments were performed with the biotin–streptavidin binding system in the integrated microfluidic device. For these experiments, biotinylated fluorescent liposomes (with SRB dye in the core and bilayer) were used as the analytes to be detected. Streptavidin-coated magnetic beads immobilized in the channels using a permanent magnet served as the capture region. The liposomes were electrophoretically concentrated at the
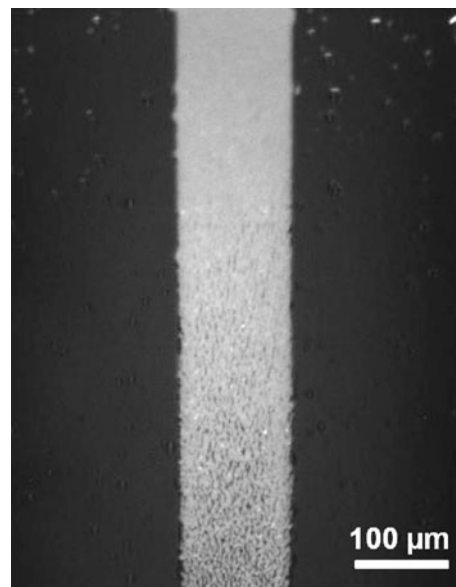

Fig. 4 Fluorescent liposomes captured at the bead bed immobilized by a permanent magnet

membrane by applying a high voltage across the membrane. The concentrated bolus of liposomes was eluted by switching the electric field toward the bead bed where the liposomes are captured. Figure 4 shows an image of the bead bed with the captured fluorescent liposomes. The unbound liposomes were washed away by flowing $1\times$ HSS as wash buffer over the bead bed. The OG solution was then injected into the channels, resulting in the lysis of the bound liposomes. The released fluorescence from the liposomes was captured downstream in the region indicated as the fluorescence measurement window in Fig. 1. Snapshots from the fluorescence burst during OG injection in the region of interest are shown in Fig. 5.

3.3 Comparison of device performance with and without concentration

In order to evaluate the effect of the preconcentration step on the performance of the system, direct injection experiments were performed in which the liposomes were injected toward the bead bed using a syringe pump bypassing the concentration step. The number of liposomes in the device was maintained the same for both sets of experiments, with and without the preconcentration step.

The total fluorescence intensity in the measurement window during OG injection was estimated from the captured videos of fluorescence burst and plotted as a function of time. These intensity profiles are shown in Fig. 6a. This figure shows data from both the electrokinetic concentration (red, color online) and direct injection (blue, color online) experiments. The area under these curves gives the integrated fluorescence intensities for each of these
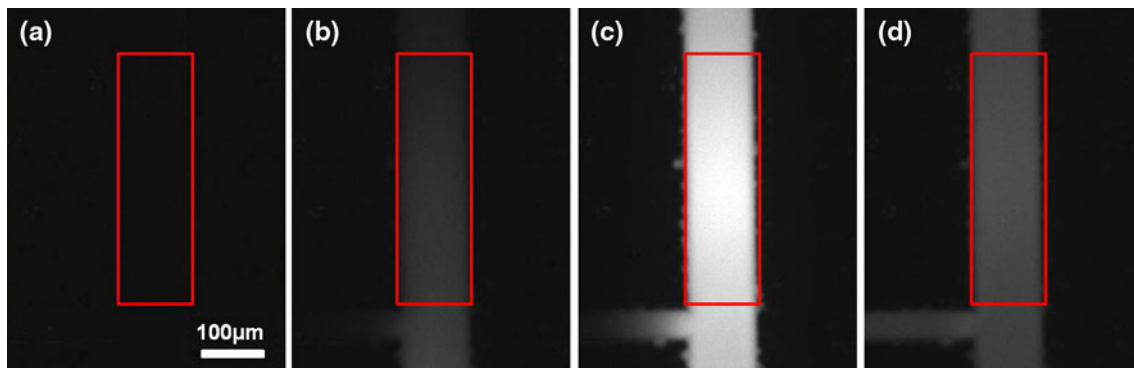
Fig. 5 Snapshots of the fluorescence measurement window (shown as a *box*) during OG injection. **a** Background image before the start of injection. **b–d** Snapshots during fluorescence burst from the lysed liposomes during OG injection
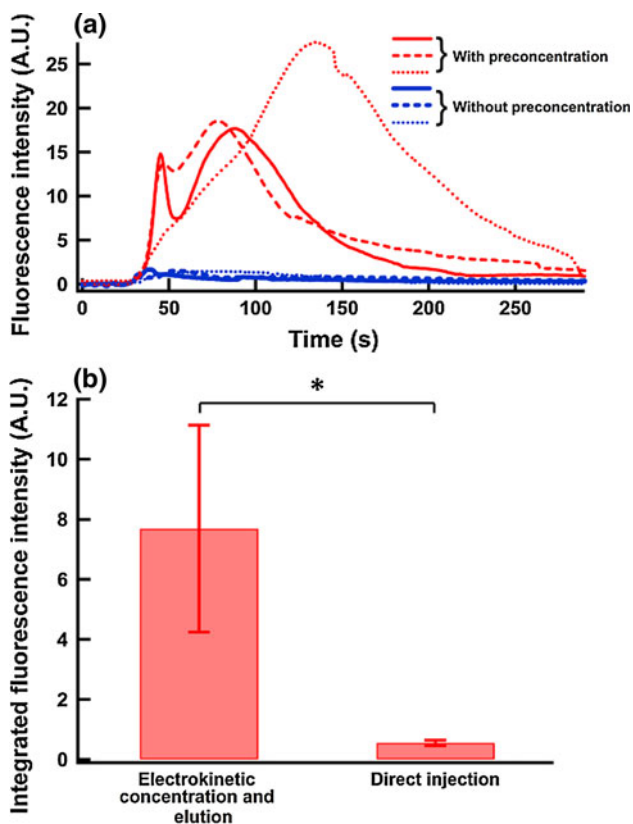

Fig. 6 a Fluorescence intensity profiles from the bead bed during OG injection for the two experiments including the preconcentration step (shown in *red lines*) and excluding it (shown in *blue lines*). **b** Comparison of the effect of preconcentration on the integrated fluorescence intensities from the bead bed during OG injection. The data is reported as mean $\pm$ SD with $n = 3$. *$P < 0.05$. (Color figure online)

experiments. These integrated intensities for the electrokinetic concentration and direct injection cases are compared in Fig. 6b. This figure shows that the inclusion of the preconcentration step increases the signal by a factor of 14. The increased signal is a result of a concentrated bolus of liposomes flowing over the bead bed resulting in better

capture efficiencies than in the case where a dilute solution of the same number of liposomes is flowed.

4 Discussion

The detection sensitivity of the biosensor depends on the binding kinetics between the low concentration of an analyte and the surface immobilized biorecognition element. This process is usually diffusion-limited (Munir et al. 2010; Sadana and Sii 1992; Kusnezow et al. 2006), and an increase in the local analyte concentration in the capture region greatly improves the binding kinetics. For molecular analytes, Singh and coworkers (Herr et al. 2007; Hatch et al. 2006) have used similar membrane-based preconcentrators in conjunction with microchip SDS-PAGE and electrophoretic immunoassays to show improved separation resolution and detection limits. Wang et al. (Wang and Han 2008) have shown 500-fold improvement in sensitivity (from 50 pM to sub 100fM) and improved dynamic range of immunoassay detection using a nanofluidic filter based electrokinetic preconcentrator. For liposomes, which are sensitive to buffer conditions and electric fields, our work reports the highest improvement in sensitivity to date.

Our design and fabrication techniques are compatible for integrating electrochemical detection into the device. The device can be operated in electrochemical detection mode by patterning gold interdigitated electrodes downstream from the membrane and using electrochemical liposomes instead of fluorescent ones (Goral et al. 2006). The low temperature bonding technique is suitable for bonding etched glass wafers with gold-patterned wafers as it does not lead to delamination of the gold electrodes as often seen in the conventional high temperature bonding techniques. Also, the core of the liposomes can be filled with electrochemical species such as potassium ferri/ferro hexacyanide molecules instead of fluorophores for detection. This straightforward extension to an electrochemical system is

advantageous as electrochemical detection methods offer several benefits over popularly used optical detection techniques. These include low capital cost for equipment, portability, low power requirement, and lack of photobleaching issues (Kwakye et al. 2006; Kwakye and Baeumner 2007).

In conclusion, we have presented an integrated microfluidic biosensor that integrates on-chip concentration with liposome-based signal amplification on the same device. We have achieved two orders of magnitude concentration with the membrane-based system within 160 s of applying high voltage across the membrane. The electric field can be switched to elute the concentrated sample bolus toward the detection region where it is captured efficiently at the immobilized bead bed. The inclusion of the preconcentration step results in a 14-fold improvement in the signal as opposed to a system without the preconcentration step, when the same number of liposomes is introduced in both cases. The functionality of the membrane can be extended to a filtering device for removing small interfering particles that competitively bind to the target probes, further increasing the signal-to-noise ratio. The inclusion of the preconcentration system in the integrated device along with the post-binding amplification achieved using liposomes help to improve the limit of detection of the biosensor. By extending the biosensor operation to electrochemical detection format, we can build an inexpensive and portable system that can be used pathogen detection.

References

Arora A, Simone G, Salieb-Beugelaar GB, Kim JT, Manz A (2010) Latest developments in micro total analysis systems. Anal Chem 82(12):4830–4847

Beyor N, Yi L, Seo TS, Mathies RA (2009) Integrated capture, concentration, polymerase chain reaction, and capillary electrophoretic analysis of pathogens on a chip. Anal Chem 81(9): 3523–3528

Cabrera CR, Yager P (2001) Continuous concentration of bacteria in a microfluidic flow cell using electrokinetic techniques. Electrophoresis 22(2):355–362

Chen L, Manz A, Day PJR (2007) Total nucleic acid analysis integrated on microfluidic devices. Lab Chip 7(11):1413–1423

Easley CJ, Karlinsey JM, Bienvenue JM, Legendre LA, Roper MG, Feldman SH, Hughes MA, Hewlett EL, Merkel TJ, Ferrance JP, Landers JP (2006) A fully integrated microfluidic genetic analysis system with sample-in-answer-out capability. Proc Natl Acad Sci USA 103(51):19272–19277

Edwards K, Curtis K, Sailor J, Baeumner A (2008) Universal liposomes: preparation and usage for the detection of mRNA. Anal Bioanal Chem 391(5):1689–1702

Foote RS, Khandurina J, Jacobson SC, Ramsey JM (2005) Preconcentration of proteins on microfluidic devices using porous silica membranes. Anal Chem 77(1):57–63

Goral VN, Zaytseva NV, Baeumner AJ (2006) Electrochemical microfluidic biosensor for the detection of nucleic acid sequences. Lab Chip 6(3):414–421

Hatch AV, Herr AE, Throckmorton DJ, Brennan JS, Singh AK (2006) Integrated preconcentration SDS-PAGE of proteins in microchips using photopatterned cross-linked polyacrylamide gels. Anal Chem 78(14):4976–4984

Herr AE, Hatch AV, Throckmorton DJ, Tran HM, Brennan JS, Giannobile WV, Singh AK (2007) Microfluidic immunoassays as rapid saliva-based clinical diagnostics. Proc Natl Acad Sci USA 104(13):5268–5273

Hjerten S (1967) Free zone electrophoresis. Chromatogr Rev 9(2): 122–219

Hjerten S (1985) High-performance electrophoresis. Elimination of electroendosmosis and solute adsorption. J Chromatogr 347(2): 191–198

Holmes DL, Stellwagen NC (1991a) Estimation of polyacrylamide gel pore size from Ferguson plots of linear DNA fragments. II. Comparison of gels with different crosslinker concentrations, added agarose and added linear polyacrylamide. Electrophoresis 12(9):612–619

Holmes DL, Stellwagen NC (1991b) Estimation of polyacrylamide gel pore size from Ferguson plots of normal and anomalously migrating DNA fragments. I. Gels containing 3% N,N′-methylenebisacrylamide. Electrophoresis 12(4):253–263

Jemere AB, Oleschuk RD, Ouchen F, Fajuyigbe F, Harrison DJ (2002) An integrated solid-phase extraction system for sub-picomolar detection. Electrophoresis 23(20):3537–3544

Jung B, Bharadwaj R, Santiago JG (2003) Thousandfold signal increase using field-amplified sample stacking for on-chip electrophoresis. Electrophoresis 24(19–20):3476–3483

Jung B, Bharadwaj R, Santiago JG (2006) On-chip millionfold sample stacking using transient isotachophoresis. Anal Chem 78(7): 2319–2327

Khandurina J, Jacobson SC, Waters LC, Foote RS, Ramsey JM (1999) Microfabricated porous membrane structure for sample concentration and electrophoretic analysis. Anal Chem 71(9):1815–1819

Khandurina J, McKnight TE, Jacobson SC, Waters LC, Foote RS, Ramsey JM (2000) Integrated system for rapid PCR-based DNA analysis in microfluidic devices. Anal Chem 72(13):2995–3000

Kim SJ, Han J (2008) Self-sealed vertical polymeric nanoporous-junctions for high-throughput nanofluidic applications. Anal Chem 80(18):7179 (Erratum to document cited in CA148: 373127)

Kirby BJ, Wheeler AR, Zare RN, Fruetel JA, Shepodd TJ (2003) Programmable modification of cell adhesion and zeta potential in silica microchips. Lab Chip 3(1):5–10

Kusnezow W, Syagailo YV, Rueffer S, Klenin K, Sebald W, Hoheisel JD, Gauer C, Goychuk I (2006) Kinetics of antigen binding to antibody microspots: strong limitation by mass transport to the surface. Proteomics 6(3):794–803

Kwakye S, Baeumner A (2007) An embedded system for portable electrochemical detection. Sens Actuators B B123(1):336–343

Kwakye S, Goral VN, Baeumner AJ (2006) Electrochemical microfluidic biosensor for nucleic acid detection with integrated minipotentiostat. Biosens Bioelectron 21(12):2217–2223

Lagally ET, Scherer JR, Blazej RG, Toriello NM, Diep BA, Ramchandani M, Sensabaugh GF, Riley LW, Mathies RA (2004) Integrated portable genetic analysis microsystem for pathogen/infectious disease detection. Anal Chem 76(11): 3162–3170

Lapizco-Encinas BH, Davalos RV, Simmons BA, Cummings EB, Fintschenko Y (2005) An insulator-based (electrodeless)

dielectrophoretic concentrator for microbes in water. J Microbiol Methods 62(3):317–326

Li Y, De Voe DL, Lee CS (2003) Dynamic analyte introduction and focusing in plastic microfluidic devices for proteomic analysis. Electrophoresis 24(1–2):193–199

Lichtenberg J, Verpoorte E, de Rooij NF (2001) Sample preconcentration by field amplification stacking for microchip-based capillary electrophoresis. Electrophoresis 22(2):258–271

Liu P, Mathies RA (2009) Integrated microfluidic systems for high-performance genetic analysis. Trends Biotechnol 27(10):572–581

Mairhofer J, Roppert K, Ertl P (2009) Microfluidic systems for pathogen sensing: a review. Sensors 9(6):4804–4823

Moncada-Hernandez H, Lapizco-Encinas BH (2010) Simultaneous concentration and separation of microorganisms: insulator-based dielectrophoretic approach. Anal Bioanal Chem 396(5): 1805–1816

Munir A, Wang J, Li Z, Zhou HS (2010) Numerical analysis of a magnetic nanoparticle-enhanced microfluidic surface-based bioassay. Microfluid Nanofluid 8(5):641–652

Ohno K-I, Tachikawa K, Manz A (2008) Microfluidics: applications for analytical purposes in chemistry and biochemistry. Electrophoresis 29(22):4443–4453

Ramsey JD, Collins GE (2005) Integrated microfluidic device for solid-phase extraction coupled to micellar electrokinetic chromatography separation. Anal Chem 77(20):6664–6670

Sadana A, Sii D (1992) Binding kinetics of antigen by immobilized antibody: influence of reaction order and external diffusional limitations. Biosens Bioelectron 7(8):559–568

Siebert STA, Reeves SG, Durst RA (1993) Liposome immunomigration field assay device for alachlor determination. Anal Chim Acta 282(2):297–305

Sista R, Hua Z, Thwar P, Sudarsan A, Srinivasan V, Eckhardt A, Pollack M, Pamula V (2008) Development of a digital microfluidic platform for point of care testing. Lab Chip 8(12): 2091–2104

Song S, Singh AK, Kirby BJ (2004a) Electrophoretic concentration of proteins at laser-patterned nanoporous membranes in microchips. Anal Chem 76(15):4589–4592

Song S, Singh AK, Shepodd TJ, Kirby BJ (2004b) Microchip dialysis of proteins using in situ photopatterned nanoporous polymer membranes. Anal Chem 76(8):2367–2373

Tan W, Fan ZH, Qiu CX, Ricco AJ, Gibbons I (2002) Miniaturized capillary isoelectric focusing in plastic microfluidic devices. Electrophoresis 23(20):3638–3645

Wainright A, Williams SJ, Ciambrone G, Xue Q, Wei J, Harris D (2002) Sample pre-concentration by isotachophoresis in microfluidic devices. J Chromatogr A 979(1-2):69–80

Wang Y-C, Han J (2008) Pre-binding dynamic range and sensitivity enhancement for immuno-sensors using nanofluidic preconcentrator. Lab Chip 8(3):392–394

Wang HY, Foote RS, Jacobson SC, Schneibel JH, Ramsey JM (1997) Low temperature bonding for microfabrication of chemical analysis devices. Sens Actuators B B45(3):199–207

Wang Y-C, Stevens AL, Han J (2005) Million-fold preconcentration of proteins and peptides by nanofluidic filter. Anal Chem 77(14):4293–4299

Wang J, Zhang Y, Mohamadi MR, Kaji N, Tokeshi M, Baba Y (2009) Exceeding 20 000-fold concentration of protein by the on-line isotachophoresis concentration in poly(methyl methacrylate) microchip. Electrophoresis 30(18):3250–3256

Yu C, Davey MH, Svec F, Frechet JMJ (2001) Monolithic porous polymer for on-chip solid-phase extraction and preconcentration prepared by photoinitiated in situ polymerization within a microfluidic device. Anal Chem 73(21):5088–5096